

# Design and Optimization of Array Patch Antenna for 6G and Biomedical Applications

Siraj Younes <sup>1,\*</sup>, Foshi Jaouad <sup>1</sup>, and Saidi Alaoui Kaoutar <sup>2</sup>

<sup>1</sup>ISMSE Laboratory, Faculty of Sciences and Technology (FST) Errachidia, University of Moulay Ismail, Morocco

<sup>2</sup>Higher School of Technology Dakhla, Ibn Zohr University, Morocco

Email: sirajyounes95@gmail.com (S.Y.); j.foshi@fste.umi.ac.ma (F.J.); k.alaouisaidi@uiz.ac.ma (S.A.K.)

\*Corresponding author

**Abstract**—To improve the performance of conventional patch antennas, this paper presents the use of array strategy instead of single element. The proposed design is an array antenna with four T-shaped radiating elements optimized for on-body biomedical and 6G communication systems. The proposed design, implemented on a polyimide substrate with total size of  $100 \times 90 \times 8 \mu\text{m}^3$ , resonates at 3.77 THz, a frequency selected for its practical suitability in millimeter-scale communication links and high-resolution biomedical application. The proposed configuration also provides a clear improvement in radiation performance compared with a single-patch design. Owing to the array strategy, the antenna achieves higher gain, improved directivity, and better impedance matching while maintaining a miniaturized size. The structure achieved an  $S_{11}$  of  $-44.14$  dB, a VSWR of 1.02, a gain of 5.65 dB, and a directivity of 6.74 dB, outperforming many recently reported THz biomedical antennas of similar size. The T-shaped elements improve current distribution, while the array configuration increases gain and reduces impedance mismatch, offering a balanced solution that maintains compactness while enhancing efficiency. Performance trade-off analysis shows that although compactness slightly constrains bandwidth, the array configuration delivers substantial enhancements in gain and radiation efficiency, making it a strong candidate for future biomedical and 6G THz applications. All results were obtained using Ansys High-Frequency Structure Simulator (HFSS) and Computer Simulation Technology (CST) software.

**Keywords**—array antenna, biomedical applications, patch antenna, 6G, T-shaped, terahertz, on-body, wearable antenna, THz array

## I. INTRODUCTION

The Terahertz waves have attracted the attention of many researchers due to their numerous advantages, making them a good choice for many applications that require high-speed performance, in addition to several other applications in the medical field such as imaging and sensing. However, designing effective antennas at such high frequencies is a major challenge, as it requires designing small-sized antennas with strong radiation

characteristics that can be easily integrated with small electronic circuits.

In this research we focus on patch antennas due to their advantages such as small size, simple structure, and ease of manufacturing. This type of antennas can effectively operate at various frequencies including THz range, but they still face some limitations and problems, such as weak radiation characteristics, which hinders their performance in applications that require antennas with high performance. To address this deficiency, various solutions have been proposed recently, such as substrate modification [1], slot incorporation [2], the use of partial ground planes [3, 4], metamaterials integration [5–7], and array configurations [8, 9].

All the solutions mentioned above yielded remarkable results and improve the performance of traditional antennas, but they introduced some other problems, such as increased antenna size and more complex configurations. In this context, the array solution emerges as a suitable solution that improves antenna performance while maintaining a small size and simple configuration. This strategy relies on combining multiple elements on a single substrate, where they work together to generate a single, stronger, and more precise beam pattern. In the biomedical field, these antennas are used in various applications such as high resolution [10] bio imaging [11], cancer detection [12], and transdermal biomarker monitoring [13]. Because of the ability of terahertz waves to penetrate various biological tissues without any risk or side effects [14].

Although several THz patch antennas have been proposed for biomedical sensing and 6G short-range communication, most existing designs still suffer from insufficient gain, limited directivity, and low radiation efficiency, especially when placed in close proximity to the human body where biological tissues strongly absorb THz energy. Biomedical THz systems typically operate at very short distances (1–20 mm) with microwatt-level power, requiring antennas capable of delivering concentrated and high-quality beams to ensure reliable sensing and imaging. In THz communication links for future 6G systems, distances are generally below a few centimeters, and extremely high data rates (tens to hundreds of Gbps) demand antennas with enhanced

performance while respecting safety constraints related to tissue exposure. These challenges highlight a clear gap: the need for compact THz antennas that simultaneously provide high gain, strong directivity, and simple integration, all while operating efficiently in on-body environments.

While THz operation is often associated with post-6G theoretical research, the 3–4 THz band selected in this work is justified by its practical relevance to short-range 6G links and high-resolution biomedical sensing, where communication distances are typically very short and THz waves offer superior spatial resolution. At these frequencies, biological tissues and flexible substrates exhibit strong frequency-dependent dispersion, meaning that their permittivity and conductivity vary significantly with frequency, directly affecting impedance matching, SAR levels, and overall radiation behavior [15, 16]. Therefore, these effects are explicitly taken into account through phantom and SAR evaluations. Unlike traditional THz array patch configurations, the novel proposed array strategy combined with T-shaped radiating elements offers a more effective solution, the T-slot enhances current distribution, while the array configuration improves gain and reduces impedance mismatch, providing a realistic and application-oriented design that bridges the gap between futuristic post-6G concepts and the practical requirements of biomedical and short-range 6G communication systems.

In this research, we proposed a terahertz array antenna for medical applications as well as next-generation communications 6G. The proposed antenna showed enhanced results in terms of radiation efficiency, impedance matching, and overall efficiency, which make it a best choice for a wide range of applications. The results obtained using a single antenna and an array were compared, to confirm the array's effect in improving the traditional antenna.

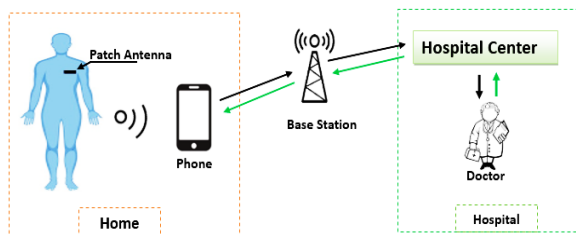


Fig. 1. Patch antenna in biomedical applications.

Fig. 1 presents the use of patch antenna in biomedical field. The patch is integrated on the human body and connected directly with some sensors designed to monitor and measure various physiological parameters, including blood pressure, glucose concentration, heart rate, and other vital body signals. The antenna receives the information collected by the sensor and then transmits it to a phone or other nearby external device. From there, the information is relayed to the hospital's central office via the internet, allowing the doctor to review it. This continuous exchange of health data enables ongoing monitoring of the patient's condition and timely intervention in case of any problem.

A first version of this work was presented in the conference paper COCIA'25 [9], and this paper represents an extended version with additional results and discussions.

## II. LITERATURE REVIEW

Recent works on high-frequency antennas can be grouped by application and operating band. For THz communication systems, a photonic-crystal-based patch array operating at 0.6 THz was presented in Ref. [17], the antenna operated at around 0.6 THz, achieving a gain of 11.6 dB, efficiency of 86.75%, and a bandwidth of 113 GHz but relying on a complex silicon crystal substrate not suitable for compact on-body use. In [8] a four-element microstrip patch array antenna was proposed using a corporate-series feed network for 5G communication systems. The antenna operates within the 25.04–30.87 GHz range, offering a wide bandwidth and a maximum gain of 9.5 dB. The design exhibits an end-fire radiation pattern, making it well suited for high frequency and directional 5G applications. Recent THz 6G antennas using graphene, meta surfaces, and EBG structures [18, 19] which provide strong gain and bandwidth but focus on free-space links and often involve large or intricate geometries.

For lower-frequency, a wideband array for high-temperature operation was proposed in Ref. [20], the design achieved a wide fractional bandwidth (~39.4%) and a peak gain of ~18.7 dBi. Additionally, the prototype was tested from  $-50^{\circ}\text{C}$  to  $+150^{\circ}\text{C}$  and demonstrated stable performance under extreme temperature variations. Moreover, a  $4 \times 4$  microstrip patch antenna for biomedical monitoring was designed in Ref. [21], achieving 17 dBi gain, with simulations in Octave and openers and directivity validated in an anechoic chamber. However, these solutions are not designed for THz on-body operation and typically prioritize robustness or far-field performance rather than ultra-compactness or integration with biological tissues.

Across these categories, key metrics such as frequency range, gain (typically 9–18 db), bandwidth, substrate type (silicon, graphene, Ku-band laminates), and on-/off-body context show that existing THz and high-frequency arrays either use complex structures, lack compact dimensions, or do not account for on-body loading and biomedical constraints. In contrast, the proposed work introduces a compact THz array patch on a thin polyimide substrate, offering enhanced gain and directivity through a simple array strategy while maintaining a very small footprint suitable for on-body biomedical and 6G scenarios

## III. SINGLE AND ARRAY ANTENNAS DESIGNS

The first proposed design is a sample T-shaped antenna, implemented on a polyimide substrate with a dielectric of 3.5, a loss tangent of 0.008, and a total size of  $48 \times 42 \times 8 \mu\text{m}^3$ . The antenna operates at 3.72 THz and exited with a feed line of  $18 \times 4 \mu\text{m}^2$ . The insertion of a T-shaped slot on the patch is used as a strategic technique to enhance the impedance matching between the patch and the feed line. The detailed structure of the single patch is presented in

Fig. 2. The initial antenna design was obtained employing the following equations, where  $C$  represents the speed of light in free space, and  $h$  denotes the substrate thickness [3]:

$$Wp = \frac{c}{2f_r} \sqrt{\frac{2}{\epsilon_{r+1}}} \quad (1)$$

$$L_{eff} = \frac{c}{2f_r \sqrt{\epsilon_{reff}}} \quad (2)$$

$$Lp = L_{eff} - 2 \Delta L \quad (3)$$

$$\Delta L = 0.412h \frac{(\epsilon_{reff}+0.3)\left(\frac{w}{h}+0.264\right)}{(\epsilon_{reff}-0.258)\left(\frac{w}{h}+0.8\right)} \quad (4)$$

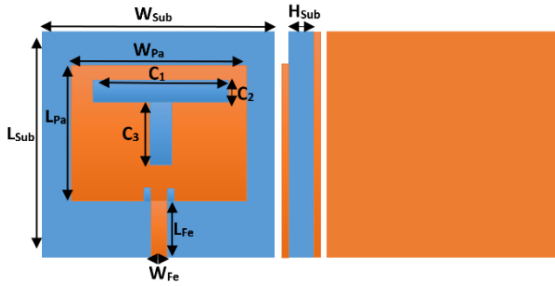


Fig. 2. Suggested antenna dimensions.

The proposed array patch antenna was developed through three iterative design stages, as illustrated in Fig. 3. After designing the single-element antenna, the configuration was extended to a two-element array, and finally, a four-element array antenna was developed.

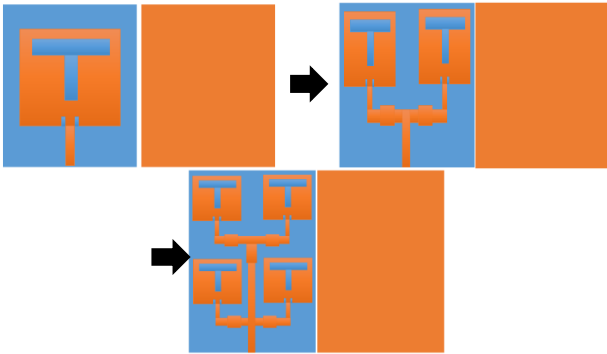


Fig. 3. Array antenna design process.

The final suggested design is detailed in Fig. 4, the antenna composed of four similar T-shaped patches, arranged on a polyimide substrate with total dimensions of  $100 \times 90 \times 8 \mu\text{m}^3$ . Four matching elements are integrated on the feed line to enhance the impedance matching and ensure uniform feeding of all array elements. The array operates at 3.77 THz, a frequency selected for its practical suitability in short-range 6G links and high-resolution biomedical applications, where THz waves offer superior spatial resolution and allow efficient on-body operation. The design achieves very good performances including increased gain, enhanced directivity and remarkable impedance matching. The single and array antennas dimensions are listed in Table I.

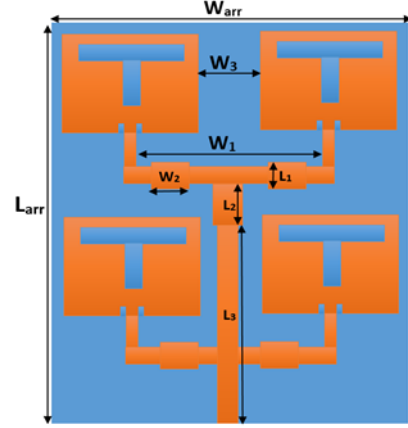


Fig. 4. Array antenna architecture.

TABLE I. ARRAY ANTENNA DIMENSIONS

Var	value ( $\mu\text{m}$ )	Var	value ( $\mu\text{m}$ )	Var	value ( $\mu\text{m}$ )
$W_{sub}$	48	C3	13	$W_1$	52
$L_{sub}$	42	$W_{fe}$	4	$W_2$	8.4
$L_{pa}$	34	$L_{fe}$	18	$L_1$	6
$W_{pa}$	25	$H_{sub}$	8	$L_2$	10
C1	24	$W_{arr}$	90	$L_3$	45
C2	4	$L_{arr}$	100	$W_3$	16

#### IV. PARAMETRIC STUDY

##### A. Effect of Substrate Type

In order to evaluate the impact of substrate material type on the antenna performance, a comparative analysis was conducted by varying the substrate types. Three substrates were considered: Rogers 5880, Silicon and polyimide. The specific electrical and physical characteristics of these materials, are presented in Table II.

TABLE II. CHARACTERISTICS OF THE INVESTIGATED SUBSTRATES

Substrate	Type	$\epsilon$	Loss Tangent	Typical operating range
Rogers 5880	Rigid	2.2	0.0009	Microwave / mmWave
Silicon	Rigid	4	0.004	THz, photonics
Polyimide	Flexible	3.5	0.008	mmWave & THz

The reflection coefficient of each type is presented in Fig. 5. All three substrates provided acceptable results across different frequencies, Rogers 5880 achieved an  $S_{11}$  of  $-12$  dB at around 4.6 THz, while silicon obtained a deeper  $S_{11}$  of  $-31$  dB at approximately 4.3 THz. However, the best performance was achieved with the polyimide substrate, exhibiting an  $S_{11}$  of  $-44$  dB at 3.77 THz.

Beyond the reflection coefficient, the influence of the substrate type on radiation characteristics was also investigated in terms of gain, directivity, and efficiency as presented in Fig. 6 and listed in Table III. The simulated realized gain is about 4.32 dB for Rogers 5880, 3.06 dB for silicon, and 5.65 dB for polyimide. The corresponding directivities are approximately 5.14 dB, 4.27 dB, and 6.74 dB, respectively. The polyimide-based design therefore

provides the highest gain and directivity among the three candidates.

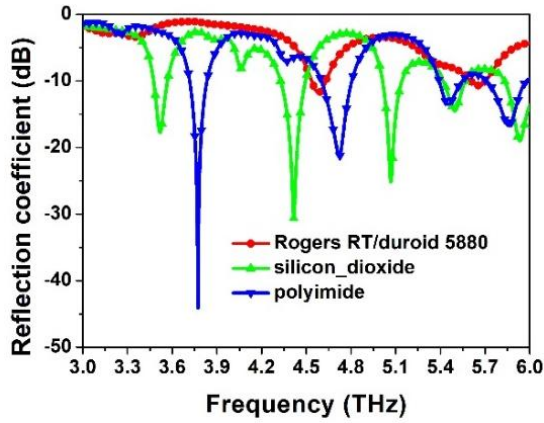
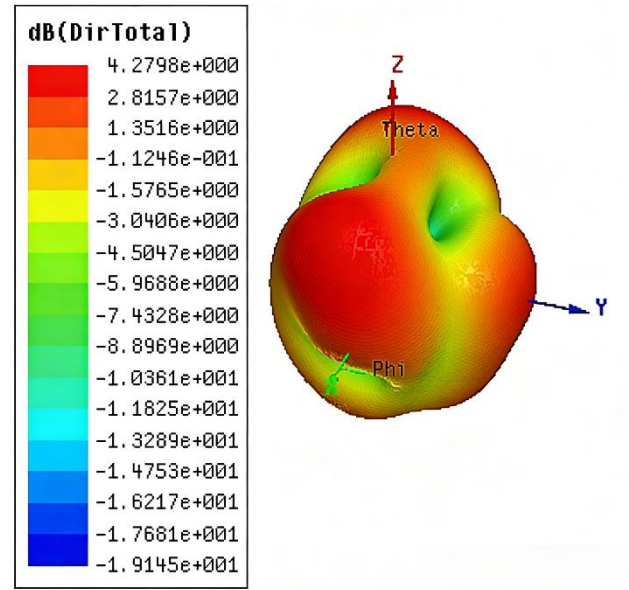
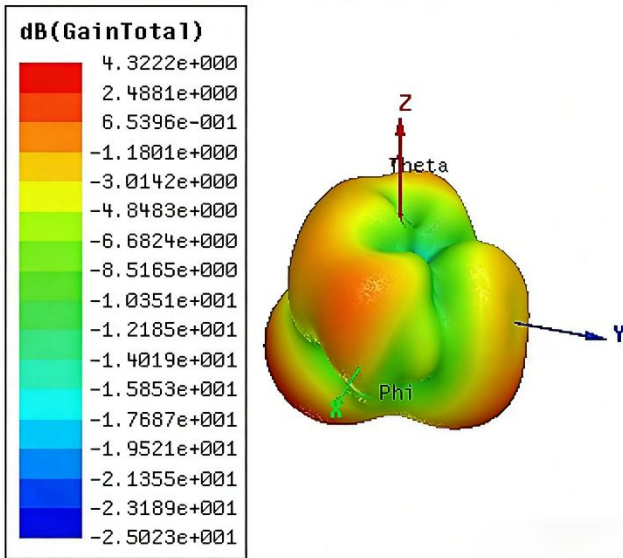
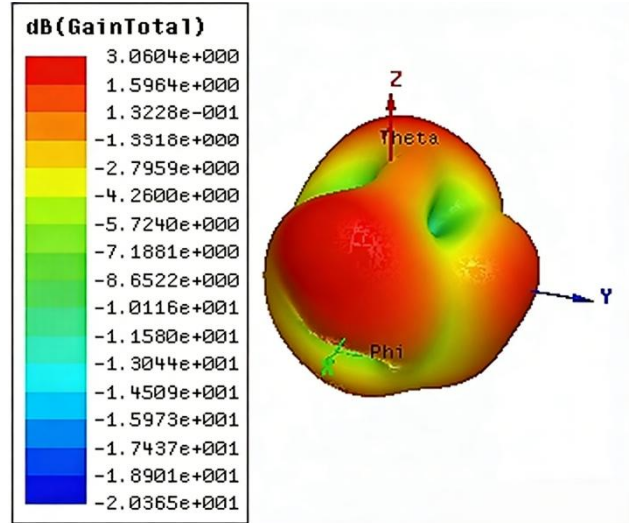


Fig. 5. Reflection coefficient with various substrates.

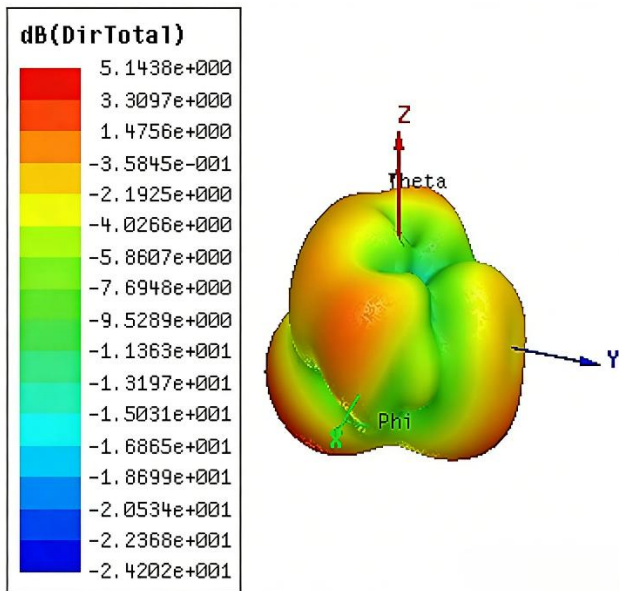


(b)

Fig. 6. Gain and directivity with (a) Rogers. (b) Silicon.

TABLE III. ANTENNA PERFORMANCE ACROSS THE THREE SUBSTRATES

Substrate	$S_{11}$ (dB)	Gain (dB)	Directivity (dB)	Efficiency
Rogers 5880	-22.13	4.32	5.14	≈ 84%
Silicon	-30.01	3.06	4.27	≈ 71.66%
Polyimide	-44.14	5.65	6.74	≈ 84%



(a)

Polyimide was selected as the final substrate because it offers the best combination of electromagnetic and biomedical suitability, its moderate permittivity and low THz loss enable superior performance, while its thin and flexible nature ensures excellent mechanical adaptability for on-body biomedical use. Unlike rigid substrates such as silicon or Rogers 5880, polyimide comfortably conforms to curved tissue surfaces, maintains stable performance under bending, and is biocompatible, making it an ideal platform for wearable THz sensing and 6G-oriented applications.

B. Effect of the Inter-element Distance  $W_3$

Another parametric study was performed to investigate the impact of the inter-elements spacing  $W_3$ . The parameter was varied from 14 to 16  $\mu\text{m}$ , in increments of 1  $\mu\text{m}$ . Fig. 7 presents the simulated  $S_{11}$ . The results confirms that the increase of spacing between the elements enhance the impedance matching by minimizing the undesired coupling. The best result is obtained with  $W_3$  of 16  $\mu\text{m}$ .

The inter-element spacing influences the level of mutual coupling between adjacent patches, which directly impacts the impedance response. At 3.77 THz, the free-space wavelength is approximately  $\lambda_0 \approx 80 \mu\text{m}$ , meaning that the tested values (14–16  $\mu\text{m}$ ) correspond to about 0.18–0.20  $\lambda_0$ . As  $W_3$  increases, the reduced electromagnetic interaction between elements leads to a more stable resonance and improved  $S_{11}$  performance. The spacing of 16  $\mu\text{m}$  provides the deepest  $S_{11}$  and the cleanest resonance because it minimizes coupling-induced perturbations while keeping the array compact.

The electric and magnetic distribution are presented in Fig. 8(a)–(b), respectively. The magnetic field (H-field) is concentrated mainly around the feed line and the conductive areas between the radiating elements with a value of  $3.5 \times 10^3 \text{ A/m}$ , indicating a good conductivity to the four elements. Additionally, electric field (E-field) showed strongest localization at the edges and apertures of each element within the array. This symmetrical distribution in the four patches promotes indicates the uniform excitation, which lead to enhanced radiation characteristics.

The field distribution directly correlates with the array’s radiation performance. The strong and uniform H-field around the feed ensures equal excitation of all patches, promoting a coherent far-field radiation pattern. The E-field localization at the patch edges and apertures, with a maximum magnitude of  $1.0 \times 10^6 \text{ V/m}$ , indicates regions of maximum surface current responsible for radiation. Together, these distributions explain the observed high gain and directivity, as the array efficiently converts the input excitation into a strong, directive THz beam.

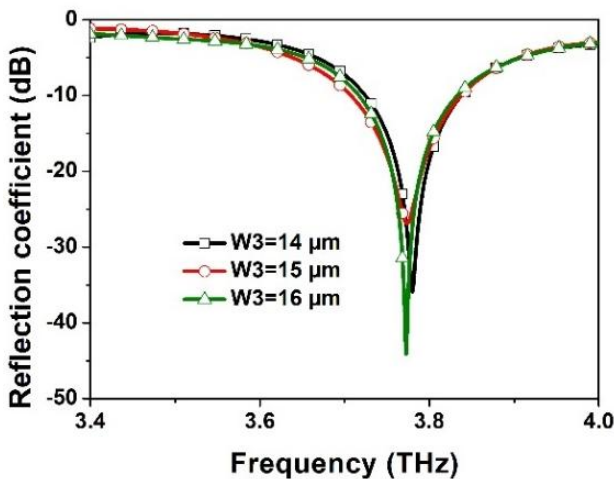


Fig. 7. Reflection coefficient with various  $W_3$  values.

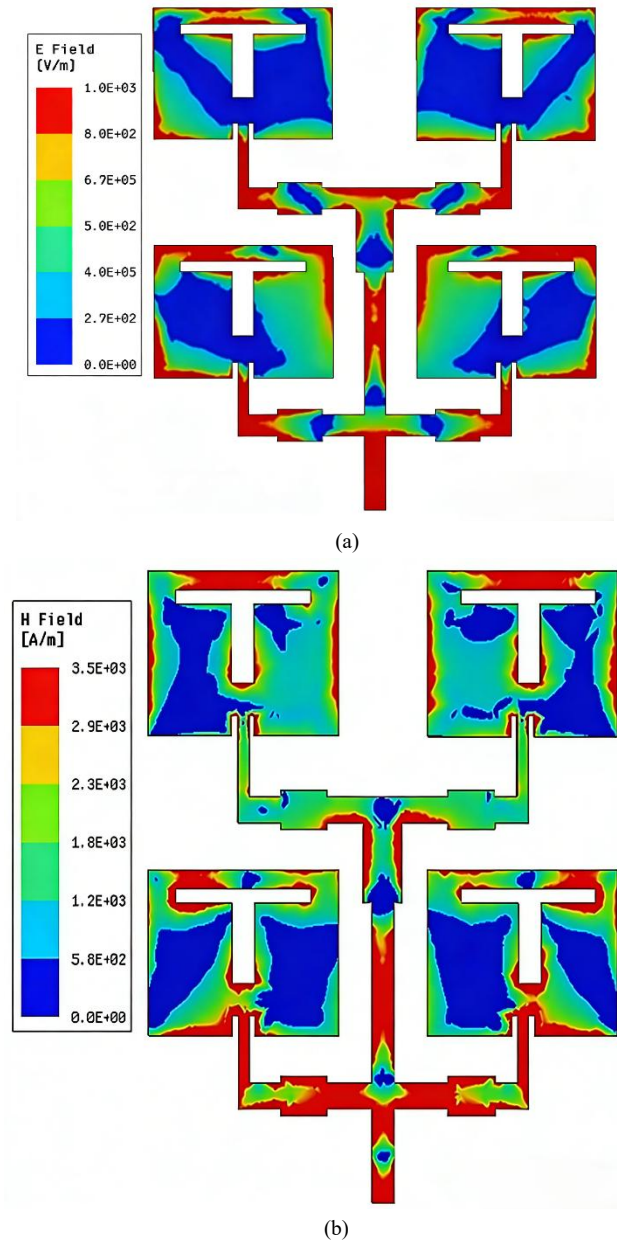


Fig. 8. Array antenna: (a) Electric, (b) Magnetic distribution.

V. RESULT AND DISCUSSION

In this section, we will discuss the obtained results, and will provides a comparison between the single and array configuration.

A. Reflection Coefficient and VSWR

The reflection coefficient and VSWR of the three design iterations are presented in Fig. 9–Fig. 10, respectively. The single element could not achieve satisfactory performance, exhibiting an  $S_{11}$  of  $-12.89 \text{ dB}$  and a  $-10 \text{ dB}$  impedance bandwidth of approximately 0.1 THz. In the second iteration, with two elements, the impedance matching was enhanced, with  $S_{11}$  decreasing to  $-24.21 \text{ dB}$  and a  $-10 \text{ dB}$  bandwidth of 0.21 THz. The optimal impedance matching was obtained with the final four elements array configuration, where the  $S_{11}$  reached its lowest value of  $-44.14 \text{ dB}$  accompanied by a bandwidth of

0.13 THz, indicating the ability of array strategy to enhance the impedance matching and minimizes the loss.

Additionally, the VSWR also improved progressively across the three design stages, starting with a value 1.2, decreased to 1.16 with  $1 \times 2$  array, and reaching an optimal value of 1.02 with the final array configuration. This improvement can be attributed to the array effect, where the combination of multiple elements enhances the effective radiating aperture, reduces mismatch at the feed, and minimizes reflection. The presence of multiple elements also allows for a more uniform current distribution and better utilization of the matching section, further widening the operational bandwidth.

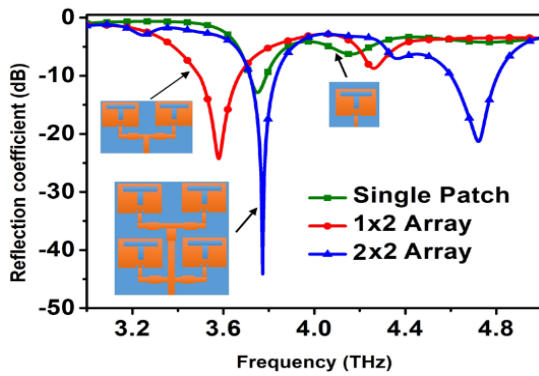


Fig. 9. Reflection coefficient of the three configurations.

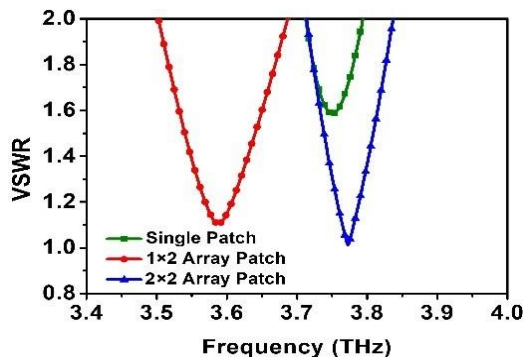
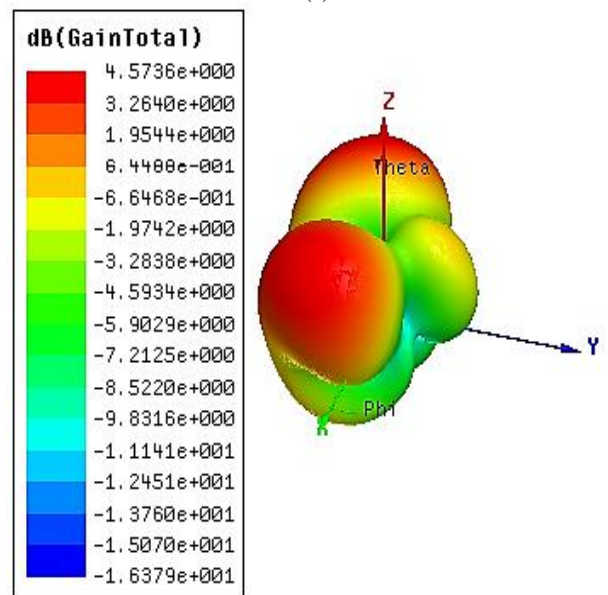
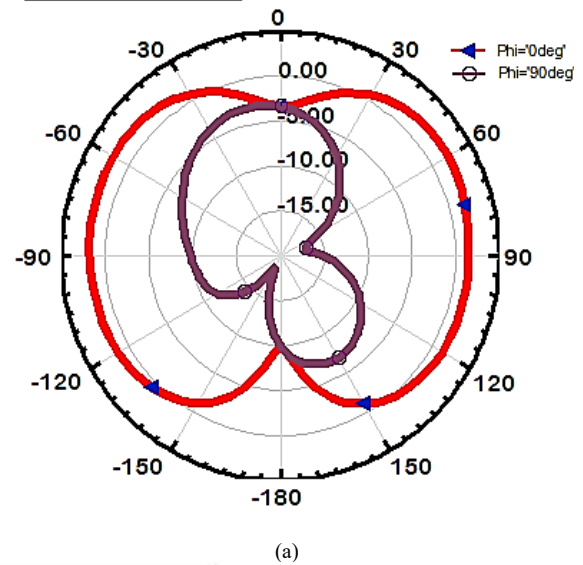
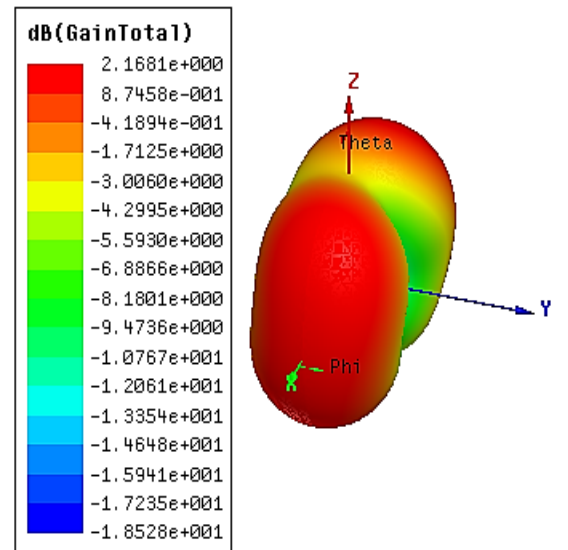


Fig. 10. VSWR of the three configurations.

### B. Radiation Patterns

The 2D and 3D gain of the three design stages are presented in Fig. 11. The gain also was enhanced across the three iterations, starting with a value of 2.16 dB as presented in Fig. 11(a). The two-elements array increased the gain to 4.57 dB (approximately by 111%) as presented in Fig. 11(b). Finally, in Fig. 11(c) the gain achieved a higher value of 5.65 dB with the four elements configuration, presenting 23% improvement over the two-element array and a total 160% enhancement compared to the single-element design. The obtained results confirm clearly the effectiveness of our proposed strategy to enhance the traditional patch antenna gain.



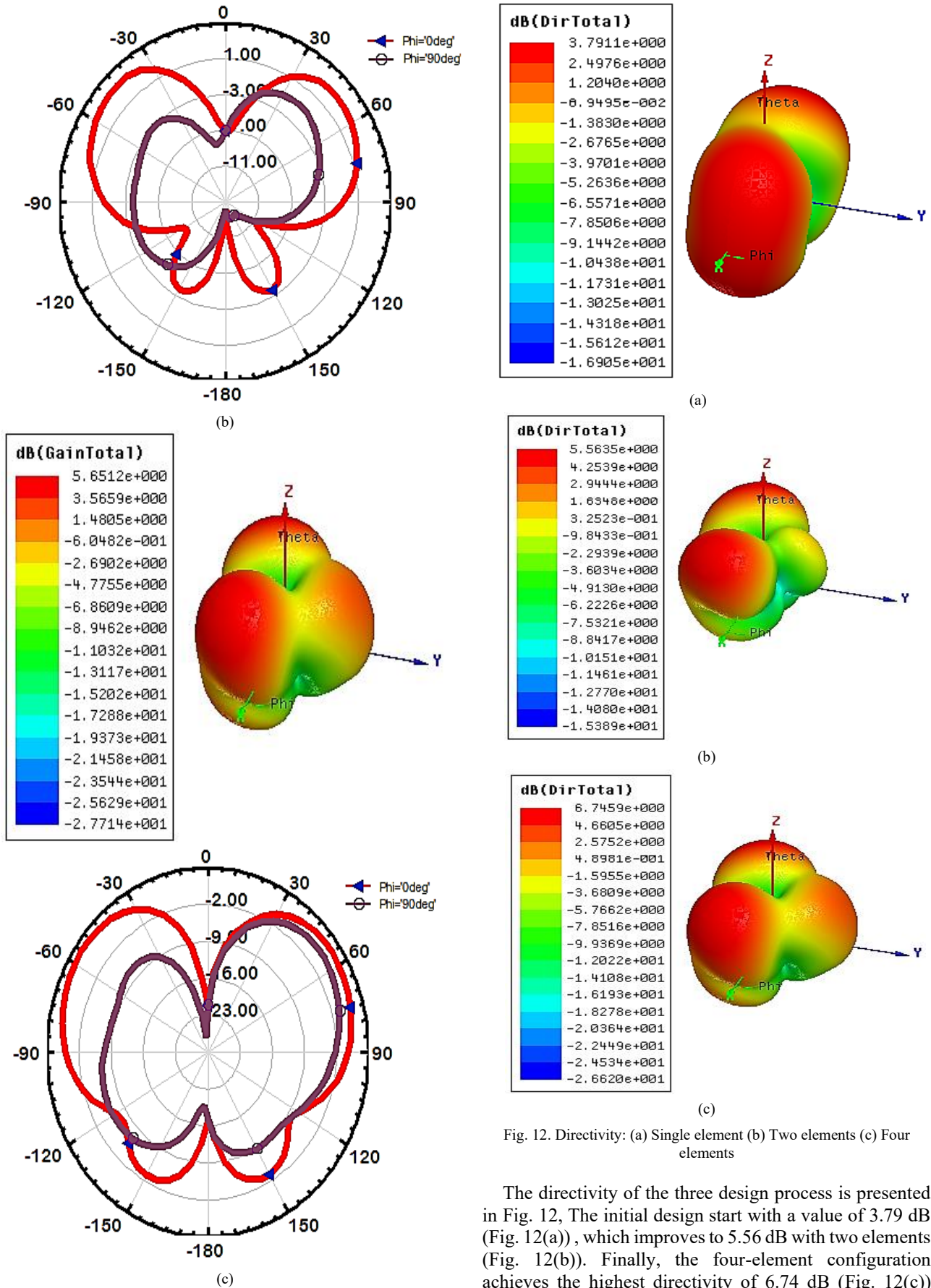


Fig. 11. 2D and 3D Radiations; (a) Single element (b) Two elements (c) Four elements.

Fig. 12. Directivity: (a) Single element (b) Two elements (c) Four elements

The directivity of the three design process is presented in Fig. 12, The initial design start with a value of 3.79 dB (Fig. 12(a)), which improves to 5.56 dB with two elements (Fig. 12(b)). Finally, the four-element configuration achieves the highest directivity of 6.74 dB (Fig. 12(c)) indicating the ability of array strategy to enhance the antenna radiation performances. The radiation

characteristics of the final array are particularly suitable for both on-body biomedical sensing and 6G communication links. The array exhibits a broadside main beam, which is ideal for off-body links where data must be transmitted efficiently from wearable or implantable sensors to nearby receivers. The moderate gain and directivity provide sufficient coverage while avoiding excessive power concentration, ensuring safe operation when placed near human tissue.

C. Simulation Near to Human Body Model

In order to evaluate the behavior of our suggested antenna in biomedical applications, we place it near to a human body model using HFSS as showed in Fig. 13. The body model consists of three layers, skin, fat, and muscle, based on standard THz tissue properties as presented in Table IV. The antenna was placed on the skin surface with a separation of 2 mm, representing a typical wearable scenario where the array is integrated into flexible electronics or a patch sensor. The obtained reflexion coefficients are presented in Fig. 14. By comparing the  $S_{11}$  on free space and on body, it is observed that the antenna retains stable impedance matching and minimal degradation in performance.

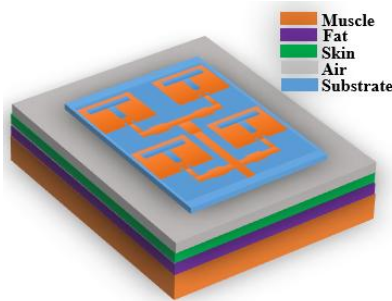


Fig. 13. Human body model.

TABLE IV. CHARACTERISTICS OF HUMAN BODY LAYERS

Layer	Skin	Fat	Muscle
Thickness(mm)	2	5	8
Permittivity	37.95	5.27	52.67
Conductivity (S/m)	1.49	0.11	1.77
Density (Kg/m <sup>3</sup> )	1001	900	1006

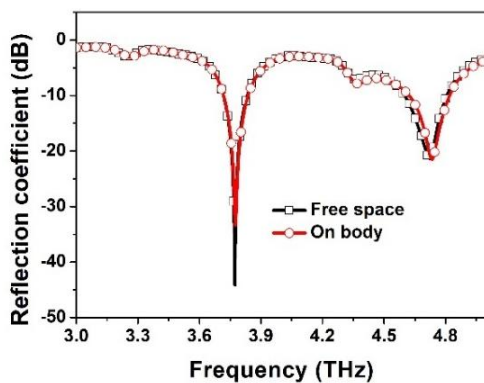


Fig. 14. Reflection coefficient in free space and on body.

As presented in Fig. 15, the radiation patterns and gain were also evaluated on-body, the maximum gain decreases

from 5.65 dB in free space to 5.40 dB on-body, while the directivity remains largely unchanged. This confirms that the antenna operates efficiently even in the presence of the lossy human tissue environment, highlighting its robustness, reliability, and strong potential for integration into wearable and biomedical sensing applications.

To ensure safety, the specific absorption rate (SAR) was calculated using CST for both 1 g and 10 g tissue volumes as showed in Fig. 16, assuming an input power of 1 mW. The maximum 1 g SAR was found to be 0.78 W/kg, and the 10 g SAR was 1.08 W/kg, both well below the IEEE/ICNIRP exposure limits of 1.6 W/kg and 2 W/kg, respectively, for localized and averaged tissue exposure. These simulations explicitly account for the frequency-dependent dispersive properties of biological tissues, which affect permittivity and conductivity and, consequently, the local SAR distribution. These results confirm compliance with safety standards and demonstrate the suitability of the proposed antenna for wearable and biomedical THz applications.

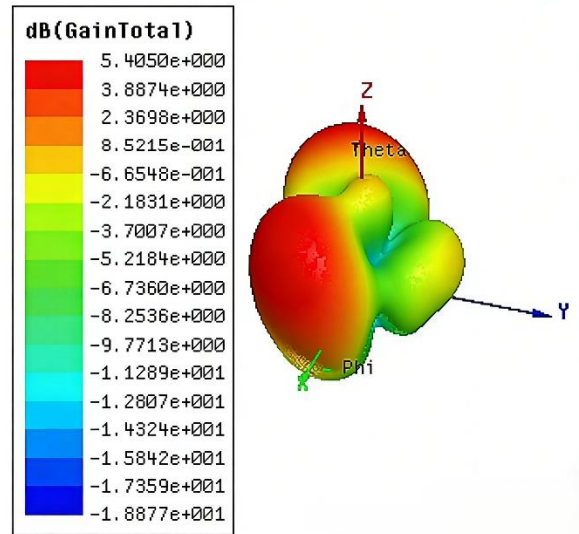
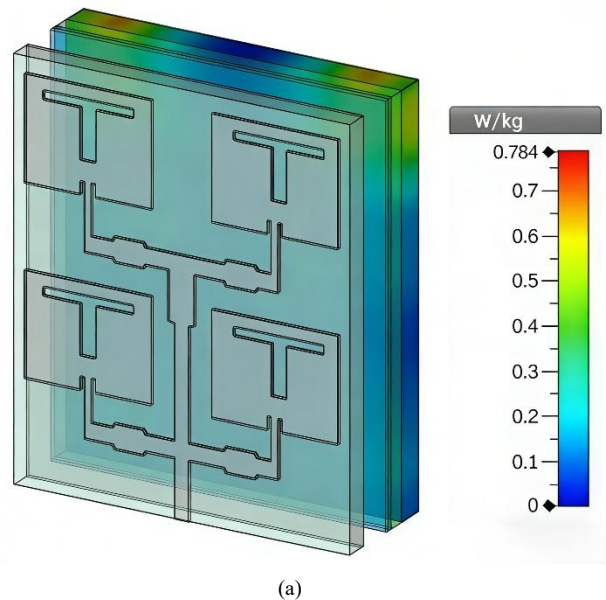


Fig. 15. 3D gain of proposed antenna with human body.



(a)

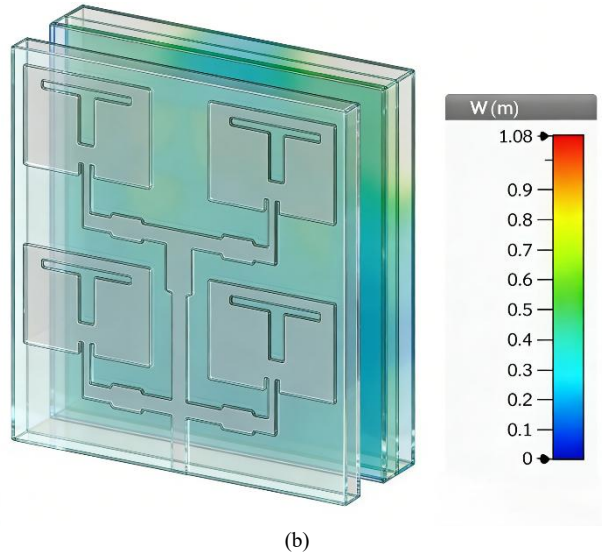


Fig. 16. SAR of the proposed array at 3.77 THz for: (a) 1 g and (b) 10 g tissue averages.

TABLE V. PERFORMANCE SUMMARY OF PROPOSED ANTENNA CONFIGURATIONS

Parameter	Single Patch	Array with two elements	Array with four elements
$S_{11}$ (dB)	-12.89	-24.21	-44.14
VSWR	1.2	1.16	1.07
Gain (dB)	2.16	4.57	5.65
Directivity (dB)	3.79	5.56	6.74

TABLE VI. COMPARISON WITH STATE OF THE ART THz ANTENNAS

Ref.	Size ( $\mu\text{m}^2$ )	Frequ (THz)	$S_{11}$ (dB)	Gain (dB)	Direct (dB)	Application
[22]	100×100	3.65	-29.00	5.01	6.06	Terahertz
[23]	30×20	3.62	-12.25	-	4.62	Terahertz
[24]	30×20	3.35	-22.00	6.03	-	Terahertz
[25]	60×54	3.73	-52.54	2.13	4	Biomedical
[26]	60×40	3.35	-45.09	5.12	4.60	Biomedical
[27]	-	3.3	-40	6.8	-	Terahertz
[Prop]	100×90	3.77	-44.14	5.65	6.74	Biomedical

Table V summarizes the obtained results, highlighting the enhancement achieved in our research. Furthermore, Table VI, provides a detailed comparison between the proposed THz antenna and the most relevant designs reported in the literature. The proposed array clearly outperforms several state-of-the-art antennas in terms of impedance matching, achieving the deepest  $S_{11}$  (-44.14 dB), which is significantly better than the values reported in Refs. [22–24]. In addition and compared with the biomedical-oriented antennas in Refs. [25, 26], the proposed array achieves similar or higher gain despite operating at a higher and more challenging THz frequency, and it offers substantially better matching performance.

## VI. CONCLUSION

In this work, a new strategy for antenna performance enhancement has been proposed by employing a multi-patch array configuration instead of a single-element design. The suggested array antenna, implemented on a polyimide substrate with a total size of  $100 \times 90 \times 8 \mu\text{m}^3$  and operating at 3.77 THz, demonstrates a significant improvement over the single-element design, the gain

increased by 160% (from 2.16 dB to 5.65 dB), the directivity improved by 78% (from 3.79 dB to 6.74 dB), and the reflection coefficient reached -44.14 dB with a VSWR of 1.02, confirming excellent impedance matching. These results highlight the strong impact of the array strategy in enhancing THz antenna performance while maintaining a compact footprint, although this approach introduces trade-offs such as potential fabrication sensitivity at the microscale. The antenna also demonstrated safe on-body operation, with a maximum 1 g SAR of 0.78 W/kg and 10 g SAR of 1.08 W/kg, both well below IEEE/ICNIRP exposure limits, confirming suitability for wearable biomedical applications. Future work will focus on the link budget calculation.

## CONFLICT OF INTEREST

The authors declare no conflict of interest.

## AUTHOR CONTRIBUTIONS

Siraj Younes conducted the research, analyzed the data, and wrote original draft; Foshi Jaouad analyzed the data, and review, validation; Saidi Alaoui Kaoutar analyzed the data, and review; all authors had approved the final version.

## REFERENCES

- [1] A. A. Abubakar and Z. Yunusa, "Comparative analysis of microstrip patch antenna on different substrate material using slit technique for x-band application," pp. 366–369 2020.
- [2] S. B. Nesar, N. Chakma, A. Mukhtadir, and A. Biswas, "Design of a miniaturized slotted T-shaped microstrip patch antenna to detect and localize brain tumor," in *Proc. 2018 International Conference on Innovations in Science, Engineering and Technology (ICISSET)*, 2018, pp. 157–162.
- [3] S. Younes and F. Jaouad, "Wearable patch antenna with rectangular slots and defected ground for biomedical applications," in *Proc. 2023 IEEE International Conference on Contemporary Computing and Communications (InC4)*, 2023, pp. 1–6.
- [4] M. L. E. Issawi, D. B. O. Konditi, and A. D. Usman, "Design of an enhanced dual-band microstrip patch antenna with defected ground structures for WLAN and WiMax," *Indonesian Journal of Electrical Engineering and Computer Science*, vol. 35, no. 1, p. 165, 2024.
- [5] A. Ahmed, V. Kumari, and G. Sheoran, "Reduction of mutual coupling in antenna array using metamaterial surface absorber," *AEU – International Journal of Electronics and Communications*, vol. 160, 154519, 2023.
- [6] H. A. A. Issa, Y. S. H. Khraisat, and F. A. S. Alghazo, "Bandwidth enhancement of microstrip patch antenna by using metamaterial," *Int. J. Interact. Mob. Technol.*, vol. 14, p.169, 2020.
- [7] P. Dawar and A. De, "Bandwidth enhancement of RMPA using ENG metamaterials at THz," in *Proc. 2013 4th International Conference on Computer and Communication Technology (ICCCCT)*, 2013, pp. 11–16.
- [8] J. Maharjan and D. Y. Choi, "Four-element microstrip patch array antenna with corporate-series feed network for 5G communication," *International Journal of Antennas and Propagation*, pp. 1–12, 2020.
- [9] S. Younes, S. A. Kaoutar, and F. Jaouad, "THz  $1 \times 4$  array patch antenna for 6G and biomedical applications," *Connected Objects, Artificial Intelligence, Telecommunications and Electronics Engineering*, vol. 1584, pp. 223–229, 2025.
- [10] M. E. Moudden, B. A. Ahmed, I. Amdaouch, M. Z. Chaari, J. R. Alzola, and O. Aghzout, "Directivity enhancement of microstrip antennas for high-resolution brain tumor imaging using characteristic modes theory and the confocal microwave image reconstruction algorithm," *e-Prime – Advances in Electrical Engineering, Electronics and Energy*, vol. 10, 100854, 2024.

- [11] D. Damyanov *et al.*, “High resolution lensless terahertz imaging and ranging,” *IEEE Access*, vol. 7, pp. 147704–147712, 2019.
- [12] R. Çalıřkan, S. S. Gültekin, D. Uzer, and Ö. Dündar, “A microstrip patch antenna design for breast cancer detection,” *Procedia - Social and Behavioral Sciences*, vol. 195, pp. 2905–2911, 2015.
- [13] F. Famá *et al.*, “An IoT-based interoperable architecture for wireless biomonitoring of patients with sensor patches,” *Internet of Things*, vol. 19, 100547, 2022.
- [14] Y. Siraj, K. S. Alaoui, and J. Foshi, “Terahertz metamaterials patch antenna for high-resolution biomedical and IoT applications,” *Advances in Medical Technologies and Clinical Practice*, pp. 531–540, 2025.
- [15] E. Kunakovskaya, I. Munina, P. Turalchuk, and I. Vendik, “Propagation of electromagnetic waves through interface of biological tissue and free space,” in *Proc. 2016 IEEE NW Russia Young Researchers in Electrical and Electronic Engineering Conference (ElConRusNW)*, 2016, pp. 767–769.
- [16] N. Vidal, S. Curto, J. M. L. Villegas, J. Sieiro, and F. M. Ramos, “Detuning study of implantable antennas inside the human body,” *Progress in Electromagnetics Research*, vol. 124, pp. 265–283, 2012.
- [17] M. E. Benlakehal, A. Hocini, D. Khedrouche, M. N. E. Temmar, and T. A. Denidni, “Design and analysis of novel microstrip patch antenna array based on photonic crystal in THz,” *Opt. Quant Electron*, vol. 54, p. 297, 2022.
- [18] M. E. Mousa, R. H. Elabd, A. J. A. A. Gburi, and A. A. Megahed, “High-gain graphene terahertz MIMO antenna with metasurface and electromagnetic bandgap for 6G applications,” *Diamond and Related Materials*, vol. 161, 113054, 2026.
- [19] A. Armghan, S. K. Patel, S. Lavadiya, K. Aliqab, and M. Alsharari, “Graphene-based four-corner meandered slotted THz antenna design for 6G/TWPAN high speed wireless communication devices,” *Ain Shams Engineering Journal*, vol. 16, 103542, 2025.
- [20] R. Li *et al.*, “Design of wideband high-gain patch antenna array for high-temperature applications,” *Sensors*, vol. 23, 3821, 2023.
- [21] V. E. Monda *et al.*, “High gain patch antenna array for biomedical applications,” in *Proc. 2022 International Conference and Exposition on Electrical and Power Engineering (EPE)*, 2022, pp. 152–156.
- [22] M. Zubair, A. Jabbar, M. O. Akinsolu, M. A. Imran, B. Liu, and Q. H. Abbasi, “Design of truncated microstrip square patch antenna for terahertz communication,” in *Proc. 2022 IEEE International Symposium on Antennas and Propagation and USNC-URSI Radio Science Meeting*, 2022, pp. 1558–1559.
- [23] Z. Mezache, “Analysis of multiband graphene-based terahertz square-ring fractal antenna,” *Ukr. J. Phys. Opt.*, vol. 21, no. 2, pp. 93–102, 2020.
- [24] J. N. George and M. G. Madhan, “Analysis of single band and dual band graphene-based patch antenna for terahertz region,” *Physica E: Low-dimensional Systems and Nanostructures*, vol. 94, pp. 126–131, 2017.
- [25] T. Hossain, M. Parvez, A. Z. M. Imran, M. J. Uddin, A. Gafur, and S. Z. Rashid, “TeraHertz antenna for biomedical application,” in *Proc. 2022 International Conference on Innovations in Science, Engineering and Technology (ICISSET)*, 2022, pp. 42–45.
- [26] P. G. Kaur, V. Mehta, and E. Sidhu, “Rectangular terahertz microstrip patch antenna design for vitamin K2 detection applications,” in *Proc. 2017 1st International Conference on Electronics, Materials Engineering and Nano-Technology*, 2017, pp. 1–3.
- [27] M. S. Gilan, J. R. Mohassel, M. N. Moghaddasi, and M. Khatir, “Design of a wideband microstrip nanoantenna array,” *Opt. Quant Electron*, vol. 51, p. 132, 2019.

Copyright © 2026 by the authors. This is an open access article distributed under the Creative Commons Attribution License which permits unrestricted use, distribution, and reproduction in any medium, provided the original work is properly cited ([CC BY 4.0](https://creativecommons.org/licenses/by/4.0/)).